Supporting Information for

Joint Inversion of Summertime Anthropogenic and Biogenic NOx and NMVOC Emissions over the Continental United States Using TEMPO and TROPOMI Observations

Chia-Hua Hsu[1,2,3], Daven K. Henze[1], Arthur P. Mizzi[4,5,1], Congmeng Lyu[2,3], Rebecca H. Schwantes[3], Owen R. Cooper[3], Colin Harkins[2,3], Jian He[2,3], Meng Li[2,3], Dylan B. Millet[6], Kelley C. Wells[6], Jennifer Kaiser[7,8], Kelvin H. Bates[1], Shobha Kondragunta[9], R. Bradley Pierce[10], Colby B. Francoeur[1,2,3], Siyuan Wang[11], Gonzalo González Abad[12], Caroline R. Nowlan[12], Xiong Liu[12], Prajjwal Rawat[13,14], Carsten Warneke[3], Matthew M. Coggon[3], Chelsea E. Stockwell[3], Jeff Peischl[3], Nell B. Schafer[2,3,15], Kristen Zuraski[2,3*], Andrew D. Rollins[3], Eleanor M. Waxman[3], Lu Xu[16], Zigang Wei[9], and Brian C. McDonald[3]

[1]Department of Mechanical Engineering, University of Colorado, Boulder, CO, USA

[2]Cooperative Institute for Research in Environmental Sciences, University of Colorado, Boulder, CO, USA

[3]NOAA Chemical Sciences Laboratory, Boulder, CO, USA

[4] NASA Earth Exchange, NASA Ames Research Center, Moffett Field, CA, USA

[5]Bay Area Environmental Research Institute, Moffett Field, CA, USA

[6]Department of Soil, Water, and Climate, University of Minnesota, St. Paul, MN, USA

[7]School of Civil and Environmental Engineering, Georgia Institute of Technology, Atlanta, GA, USA

[8]School of Earth and Atmospheric Sciences, Georgia Institute of Technology, Atlanta, GA, USA

[9]NOAA/NESDIS/Center for Satellite Applications and Research, College Park, MD, USA

[10]Space Science and Engineering Center, University of Wisconsin-Madison, Madison, WI, USA

[11]Rosenstiel School of Marine, Atmospheric, and Earth Science, University of Miami, Miami, FL, USA

[12]Atomic and Molecular Physics Division, Center for Astrophysics | Harvard & Smithsonian, Cambridge, MA, USA

[13]Hampton University, Hampton, VA, USA

[14]NASA Langley Research Center, Hampton, VA, USA

[15]Department of Chemistry, University of Colorado Boulder, Boulder, CO, USA

[16]Department of Energy, Environmental and Chemical Engineering, Washington University in St. Louis, St. Louis, MO, USA

*now at Google Quantum AI, Boulder, CO USA

Contents of this file

Text S1
Figures S1-S5
Table S1-S3

Text S1: Description and example of NMVOCs emissions optimization procedure

We aggregated individual NMVOC emissions into seven groups and optimized the lumped emissions in bulk using the satellite HCHO data. For anthropogenic NMVOC emissions, we lumped the indivudual species based on the chemical compound's functional group into alkanes, alkenes, aldehydes, alcohols, ketones, aromatics, other anthropogenic NMVOCs groups. The biogenic NMVOCs emissions, excepting biogenic isoprene, are aggregated for inversion. The species within each NMVOCs emissions group and their definition is provided in Table S2.

Once the posterior emissions are dervied for each NMVOC emissions group, the individual species within the group is updated by applying the emissions scaling factor calculated from the aggregated emissions, and we use emissions of the alkane group to illustrate this process. The emissions scaling factor is defined in Eq (S1) at each DA cycle:

$$S^j_{alkane} = E_a^j_{alkane} / E_p^j_{alkane} \quad (S1)$$

The S^j_{alkane} represent a 3-D scaling factor (emissions adjustment) for each ensemble member j, $E_a^j_{alkane}$ and $E_p^j_{alkane}$ are the posterior and prior total alkane emissions value for each ensemble j. The individual emissions species within the alkane group are then updated as:

$$E_a_i^j = E_p_i^j \times S^j_{alkane}, i = NMVOCs\ species\ within\ alkane\ group \quad (S2)$$

Where $E_a_i^j$ and $E_p_i^j$ represent each member of the posterior and prior emissions value from individual NMVOC emissions (e.g., E_ETH, E_HC3, E_HC5, and E_HC8) in alkane group. This approach propogates the emissions adjustment from the group NMVOCs level down to individual emissions species. However, we also noticed that this scaling approach could introduce additional spread into NMVOC emissions. To maintain a stable ensemble spread for long term simulation, using the esemble mean of the posterior and prior aggregated NMVOC emissions to define a scaling factor may be more robust (i.e., $S_{alkane} = \overline{E_a}_{alkane} / \overline{E_p}_{alkane}$).

Table S1. WRF-Chem model and data assimilation configuration.

Model Configurations	
Horizontal resolution	12 km
Vertical layers	50 (up to 50 hPa)
MET and CHEM IC/BC	NCEP North American Mesoscale (NAM, https://rda.ucar.edu/datasets/ds609.0) Analysis & Realtime Air Quality Modeling System (RAQMS, http://raqms-ops.ssec.wisc.edu/) (Pierce et al., 2003)
Anthropogenic emissions	GRA^{2}PES (based on 2023)
Biogenic emissions	BEIS3.14
Fire emissions	Regional hourly Advanced Baseline Imager and the Visible Infrared Imaging Radiometer Suite Emissions (RAVE)
Planetary boundary layer	Mellor-Yamada Nakanishi and Niino level 2.5 (Nakanishi and Niino, 2004)
Surface layer	Mellor-Yamada Nakanishi and Niino (Nakanishi and Niino, 2004)
Land surface	Noah land surface model (Mukul Tewari et al., 2004)
Microphysics	WRF single moment 5-class (Hong et al., 2004)
Cumulus scheme	Grell-Devenyi (GD) ensemble cumulus (Grell and Dévényi, 2002)
Short- and long-wave radiation	Rapid radiative transfer model for general circulation models (Mlawer et al., 1997)
Photolysis	Madronich photolysis (TUV)
Gas-phase chemistry	RACM2B_VCP (chem_opt=113)
Aerosol-phase chemistry	MADE/VBS
Lightning flash rate	Cloud-top height for parameterized convection
Lightning parameters	Flashrate_factor = 1; cloud top adjustment = 0
Lightning NO_x production rate	125 moles/flash for intra-cloud (IC) and cloud-ground (CG)
IC: CG ratio	Prescribed climatological based on Boccippio et al., 2001
Data assimilation configurations	
Filter type	EAKF
Ensemble members	20
DA cycle	3-hours
DA window	±1.5hr (TROPOMI), ±0.5hr (TEMPO), ±1.5 hr (Meteorological observations)
Inflation	adaptive inflation (Anderson, 2007)
Inflation damping	0.65
horizontal (vertical) localization half-width radius for CHEM OBS	38 km (off)
horizontal (vertical) localization half-width radius for MET OBS	150 km (1km)
chemical ICs/BCs and emissions uncertainty	30%
temporal correlation length	24 (Chem ICs/BCs) and 72 (Emissions) hours

Table S2. NMVOCs emissions and groups definition.

NMVOCs Emissions Group	Emissions Species
Alkanes	E_ETH, E_HC3, E_HC5, E_HC8
Alkenes	E_OL2, E_OLI, E_OLT, E_TERP, E_ISO, E_DIEN
Aldehydes	E_HCHO, E_MACR, E_CUALD, E_GLY, E_MGLY, E_ACD, E_ALD, E_BALD, E_OALD, E_CALD, E_NALD
Alcohols	E_EOH, E_MOH, E_GLYC, E_ETEG, E_PROG, E_IPOH
Ketones	E_ACT, E_MEK, E_KET, E_MVK
Aromatic	E_TOL, E_XYL, E_XYO, E_PHEN, E_BEN, E_CSL, E_MCT
Other	E_ORA1, E_ORA2, E_ACE, E_D4SILX, E_D5SILX
biogenic isoprene	SEBIO_ISO
Other biogenic NMVOC	SEBIO_MOH, SEBIO_API, SEBIO_LIM, SEBIO_MBO, SEBIO_SESQ, SEBIO_KET, SEBIO_ALD, SEBIO_EOH, SEBIO_HC3, SEBIO_ETH, SEBIO_OLI, SEBIO_OLT, SEBIO_ETE, SEBIO_XYL, SEBIO_HCHO, SEBIO_ACT, SEBIO_ACD, SEBIO_ORA1, SEBIO_ORA2, SEBIO_ECLP

Emission Name	Definition
E_ETH	Ethane
E_HC3	Alkanes, esters and alkynes with OH rate constant < 3.4x10-12 cm3 s-1
E_HC5	Alkanes, esters and alkynes with OH rate constant between 3.4x10-12 and 6.8x10-12 cm3 s-1
E_HC8	Alkanes, esters and alkynes with OH rate constant > 6.8x10-12 cm3 s-1
E_OL2	Ethene (Ethylene)
E_OLI	Internal alkenes
E_OLT	Terminal alkenes
E_TERP	Monoterpenes (alpha-pinene, d-limonene, etc.)
E_ISO	Isoprene
E_DIEN	Butadiene and other anthropogenic dienes
E_HCHO	Formaldehyde
E_MACR	Methacrolein
E_CUALD	Unsaturated aldehydes
E_GLY	Glyoxal
E_MGLY	Methylglyoxal and other alpha-carbonyl aldehydes
E_ACD	Acetaldehyde
E_ALD	C3 and higher aldehydes
E_BALD	Benzaldehyde and other aromatic aldehydes
E_OALD	Other higher aldehydes

E_CALD	Crotonaldehyde and other higher unsaturated aldehydes
E_NALD	Nitrooxyacetaldehyde
E_IPOH	Isopropanol (Isopropyl alcohol)
E_EOH	Ethanol
E_MOH	Methanol
E_GLYC	Glycerol
E_ETEG	Ethylene glycol
E_PROG	Propylene glycol
E_ACT	Acetone
E_MEK	Methyl ethyl ketone
E_KET	C5 and higher ketones
E_MVK	Methyl vinyl ketone
E_TOL	Toluene and less reactive aromatics
E_XYL	m-Xylene / p-Xylene
E_XYO	o-Xylene
E_PHEN	Phenol
E_BEN	Benzene
E_CSL	Cresol and other hydroxy substituted aromatics
E_MCT	Methyl catechol
E_ORA1	Formic acid
E_ORA2	Acetic acid and higher acids
E_ACE	Acetylene
E_D4SILX	D4-Siloxane (Octamethylcyclotetrasiloxane)
E_D5SILX	D5-Siloxane (Decamethylcyclopentasiloxane)

Table S3. Pandora sites used in this study.

Site Name	Site number	NO_2	HCHO	Latitude	Longitude
GreenbeltMD	2	x	x	38.99	-76.84
HoustonTX	25	x		29.72	-95.34
CharlesCityVA	31	x	x	37.33	-77.21
GreenbeltMD	32		x	38.99	-76.84
MountainViewCA	34	x	x	37.42	-122.06
BayonneNJ	38	x	x	40.67	-74.13
DearbornMI	39	x	x	42.31	-83.15
OldFieldNY	51	x	x	40.96	-73.14
RichmondCA	52	x	x	37.91	-122.34
BoulderCO	57	x	x	39.99	-105.26
AldineTX	61	x	x	29.90	-95.33
NewHavenCT	64	x		41.30	-72.90
HuntsvilleAL	66	x	x	34.73	-86.65
WrightwoodCA	68	x		34.38	-117.68
NewBrunswickNJ	69	x	x	40.46	-74.43
ChapelHillNC	70	x	x	35.97	-79.09
SaltLakeCityUT-Hawthorne	72	x	x	40.73	-111.87
EdwardsCA	74	x		34.96	-117.88
BeltsvilleMD	80	x		39.06	-76.88
Toronto-West	108	x		43.71	-79.54
BristolPA	134	x	x	40.11	-74.88
ManhattanNY-CCNY	135	x		40.82	-73.95
SouthJordanUT	139	x		40.55	-112.07
WashingtonDC	140	x	x	38.92	-77.01
MexicoCity-UNAM	142	x	x	19.33	-99.18
Toronto-Scarborough	145	x	x	43.78	-79.19
SWDetroitMI	147	x	x	42.30	-83.11
SaltLakeCityUT	154	x		40.77	-111.85
HamptonVA-HU	156	x	x	37.02	-76.34
MexicoCity-Vallejo	157	x	x	19.48	-99.15
AtlantaGA-Conyers	158	x	x	33.59	-84.07
PhiladelphiaPA	166	x	x	39.99	-75.08
AtlantaGA	173	x	x	33.78	-84.40
CornwallCT	179	x		41.82	-73.30
BronxNY	180	x	x	40.87	-73.88
SanJoseCA	181	x		37.33	-121.88
LondonderryNH	183	x		42.86	-71.38
CapeElizabethME	184	x		43.56	-70.21
EastProvidenceRI	185	x	x	41.84	-71.36
MadisonCT	186	x	x	41.26	-72.55
PittsburghPA	187	x	x	40.47	-79.96

GrandForksND	200	x		47.92	-97.09
BoulderCO-NCAR	204	x	x	40.04	-105.24
BuffaloNY	206	x	x	43.00	-78.79
ArlingtonTX	207	x	x	32.73	-97.11
Windsor-West	208	x	x	42.29	-83.07
NewLondonCT	236	x		41.38	-72.10
AtlantaGA-SouthDeKalb	237	x	x	33.78	-84.40
WhittierCA	247	x		33.98	-118.03
TurlockCA	248	x	x	37.52	-120.86
ChicagoIL	249	x	x	41.97	-87.71
TylerTX	259	x	x	32.34	-95.42
CameronLA	260	x	x	29.79	-93.11

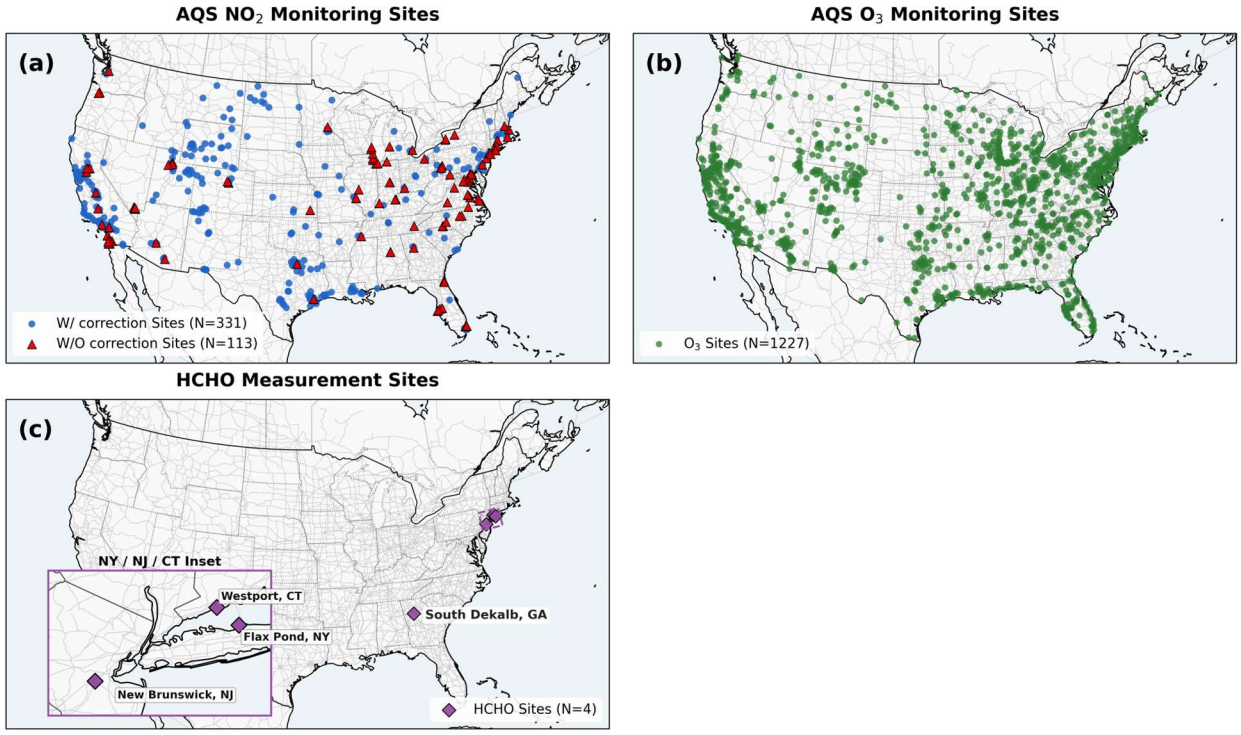


Figure S1. AQS site map for (a) NO_2, (b) O_3, and (c) HCHO. The NO_2 observations sites shown in blue circles are corrected.

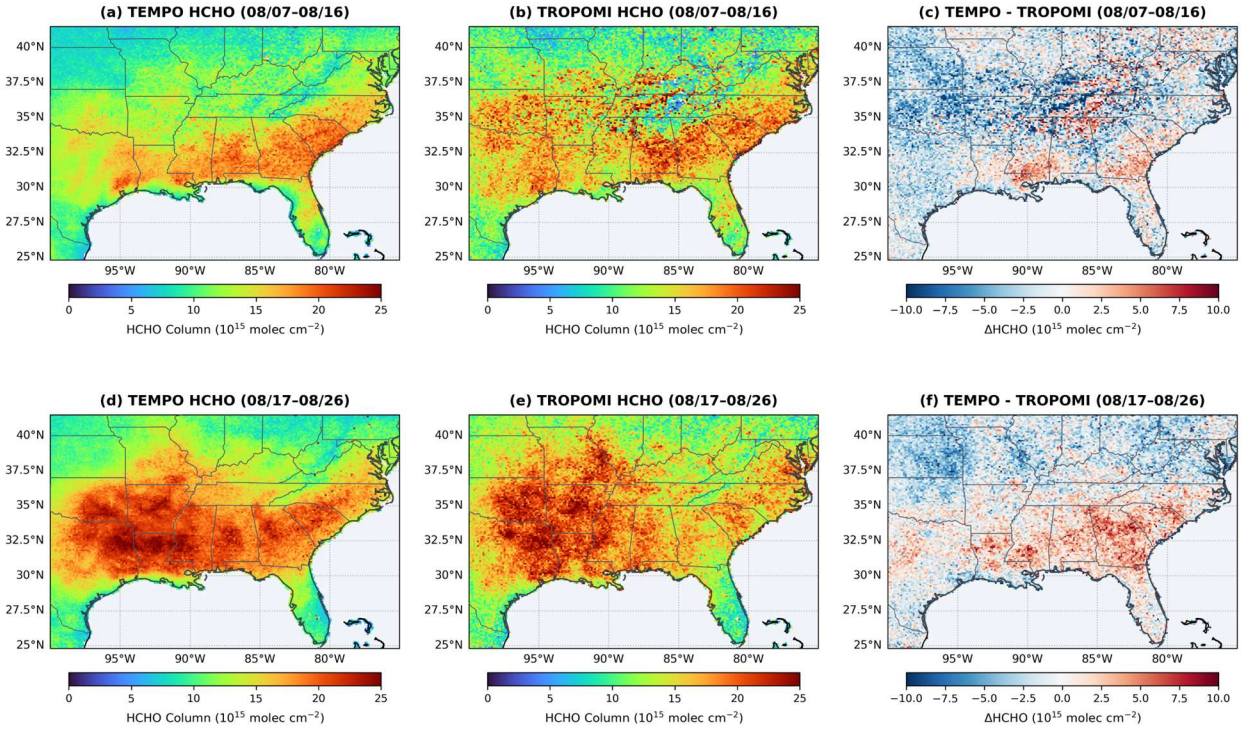


Figure S2. Comparison of averaged TEMPO and TROPOMI HCHO columns over southeastern US during two time periods. (a)-(c) 08/07-08/16, (d)-(f) 08/17-26. The TROPOMI HCHO column shown in this image was bias corrected as described in Section 4.1.

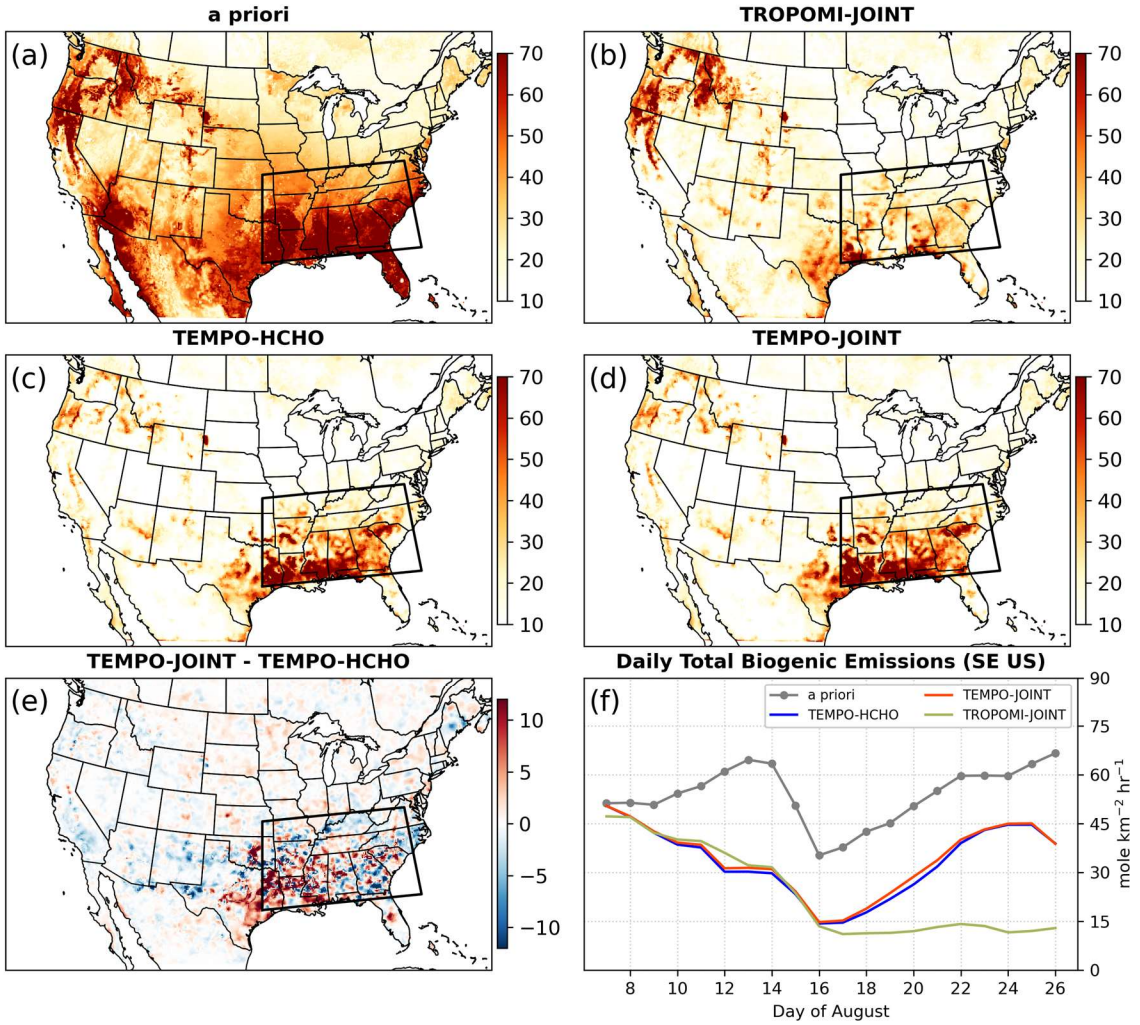


Figure S3. (a) Average other biogenic emissions spatial distribution from CTRL, (b) Average other biogenic emissions for TROPOMI-JOINT, (c) Average other biogenic emissions for TEMPO-HCHO, (d) Average other biogenic emissions for TEMPO-JOINT, (e) Difference between TEMPO-JOINT and the TEMPO-HCHO other biogenic emissions. The southeastern US is defined by the black box.

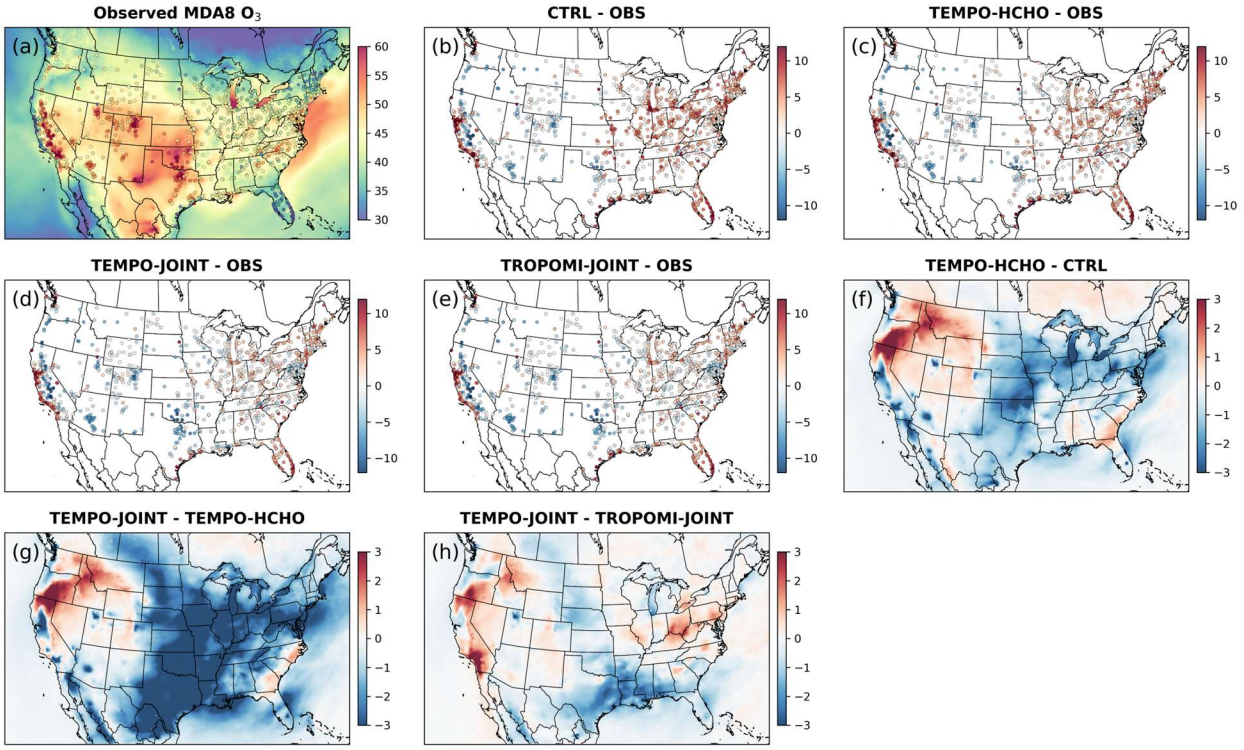
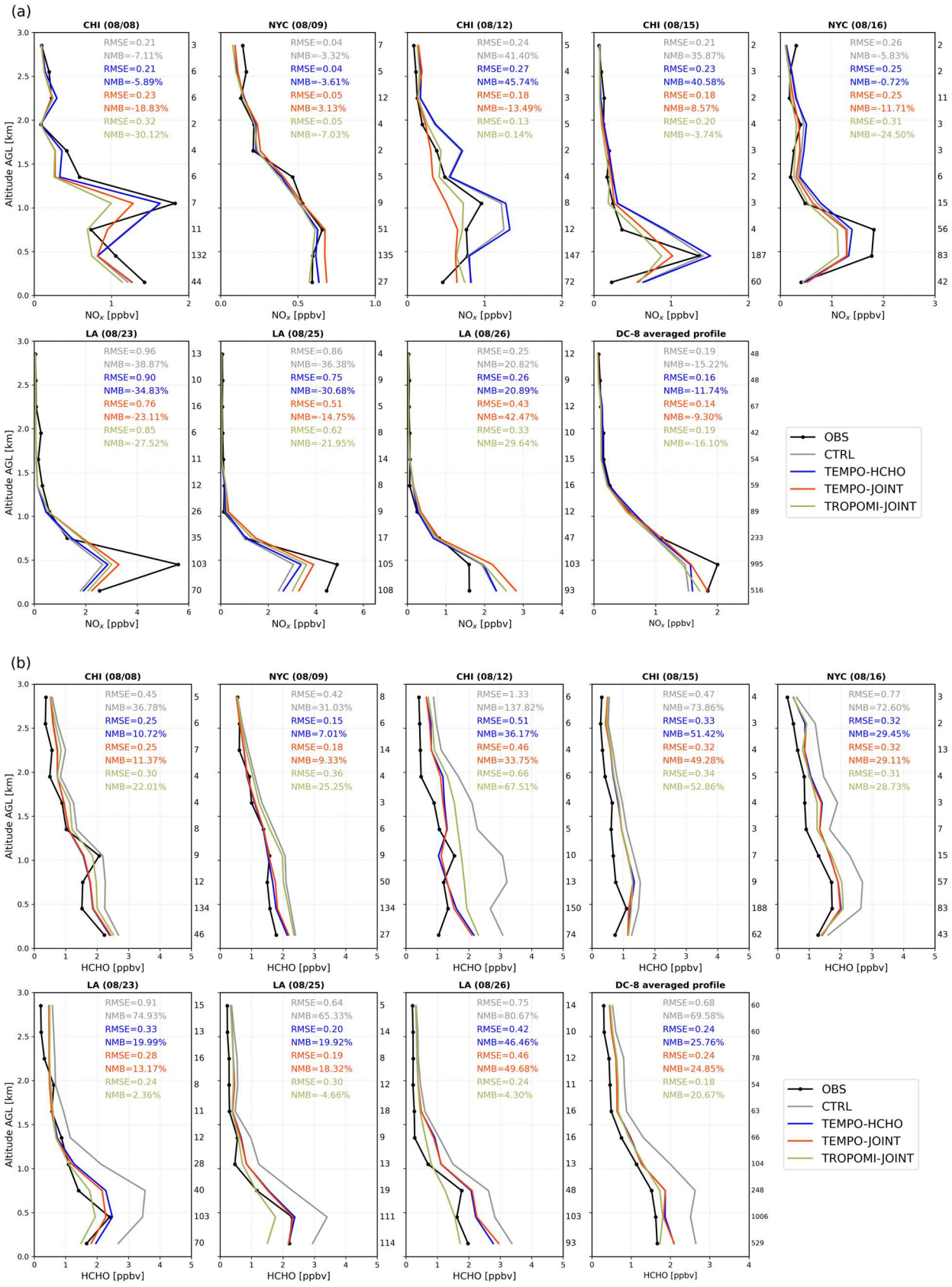


Figure S4. (a) Average AQS MDA8 O_3 overlain onto model simulated MDA8 O_3 levels, (b) Difference of MDA8 O_3 value between CTRL and AQS observations, (c) Difference of MDA8 O_3 values between TEMPO-HCHO and AQS observations, (d) Difference of MDA8 O_3 values between TEMPO-JOINT and AQS observations, (e) Difference of MDA8 O_3 values between TROPOMI-JOINT and AQS observations, (f) Difference of MDA8 O_3 values between TEMPO-HCHO and CTRL, (g) Difference of MDA8 O_3 values between TEMPO-JOINT and TEMPO-HCHO, (h) Difference of MDA8 O_3 values between TEMPO-JOINT and TROPOMI-JOINT.


(a)
CHI (08/08)
RMSE=0.21
NMB=-7.11%
RMSE=0.21
NMB=-5.89%
RMSE=0.23
NMB=-18.83%
RMSE=0.32
NMB=-30.12%
NYC (08/09)
RMSE=0.04
NMB=-3.32%
RMSE=0.04
NMB=-3.61%
RMSE=0.05
NMB=3.13%
RMSE=0.05
NMB=-7.03%
CHI (08/12)
RMSE=0.24
NMB=41.40%
RMSE=0.27
NMB=45.74%
RMSE=0.18
NMB=-13.49%
RMSE=0.13
NMB=0.14%
CHI (08/15)
RMSE=0.21
NMB=35.87%
RMSE=0.23
NMB=40.58%
RMSE=0.18
NMB=8.57%
RMSE=0.20
NMB=-3.74%
NYC (08/16)
RMSE=0.26
NMB=-5.83%
RMSE=0.25
NMB=-0.72%
RMSE=0.25
NMB=-11.71%
RMSE=0.31
NMB=-24.50%
LA (08/23)
RMSE=0.96
NMB=-38.87%
RMSE=0.90
NMB=-34.83%
RMSE=0.76
NMB=-23.11%
RMSE=0.85
NMB=-27.52%
LA (08/25)
RMSE=0.86
NMB=-36.38%
RMSE=0.75
NMB=-30.68%
RMSE=0.51
NMB=-14.75%
RMSE=0.62
NMB=-21.95%
LA (08/26)
RMSE=0.25
NMB=20.82%
RMSE=0.26
NMB=20.89%
RMSE=0.43
NMB=42.47%
RMSE=0.33
NMB=29.64%
DC-8 averaged profile
RMSE=0.19
NMB=-15.22%
RMSE=0.16
NMB=-11.74%
RMSE=0.14
NMB=-9.30%
RMSE=0.19
NMB=-16.10%
Altitude AGL [km]
NOx [ppbv]
OBS
CTRL
TEMPO-HCHO
TEMPO-JOINT
TROPOMI-JOINT
(b)
CHI (08/08)
RMSE=0.45
NMB=36.78%
RMSE=0.25
NMB=10.72%
RMSE=0.25
NMB=11.37%
RMSE=0.30
NMB=22.01%
NYC (08/09)
RMSE=0.42
NMB=31.03%
RMSE=0.15
NMB=7.01%
RMSE=0.18
NMB=9.33%
RMSE=0.36
NMB=25.25%
CHI (08/12)
RMSE=1.33
NMB=137.82%
RMSE=0.51
NMB=36.17%
RMSE=0.46
NMB=33.75%
RMSE=0.66
NMB=67.51%
CHI (08/15)
RMSE=0.47
NMB=73.86%
RMSE=0.33
NMB=51.42%
RMSE=0.32
NMB=49.28%
RMSE=0.34
NMB=52.86%
NYC (08/16)
RMSE=0.77
NMB=72.60%
RMSE=0.32
NMB=29.45%
RMSE=0.32
NMB=29.11%
RMSE=0.31
NMB=28.73%
LA (08/23)
RMSE=0.91
NMB=74.93%
RMSE=0.33
NMB=19.99%
RMSE=0.28
NMB=13.17%
RMSE=0.24
NMB=2.36%
LA (08/25)
RMSE=0.64
NMB=65.33%
RMSE=0.20
NMB=19.92%
RMSE=0.19
NMB=18.32%
RMSE=0.30
NMB=-4.66%
LA (08/26)
RMSE=0.75
NMB=80.67%
RMSE=0.42
NMB=46.46%
RMSE=0.46
NMB=49.68%
RMSE=0.24
NMB=4.30%
DC-8 averaged profile
RMSE=0.68
NMB=69.58%
RMSE=0.24
NMB=25.76%
RMSE=0.24
NMB=24.85%
RMSE=0.18
NMB=20.67%
Altitude AGL [km]
HCHO [ppbv]
OBS
CTRL
TEMPO-HCHO
TEMPO-JOINT
TROPOMI-JOINT

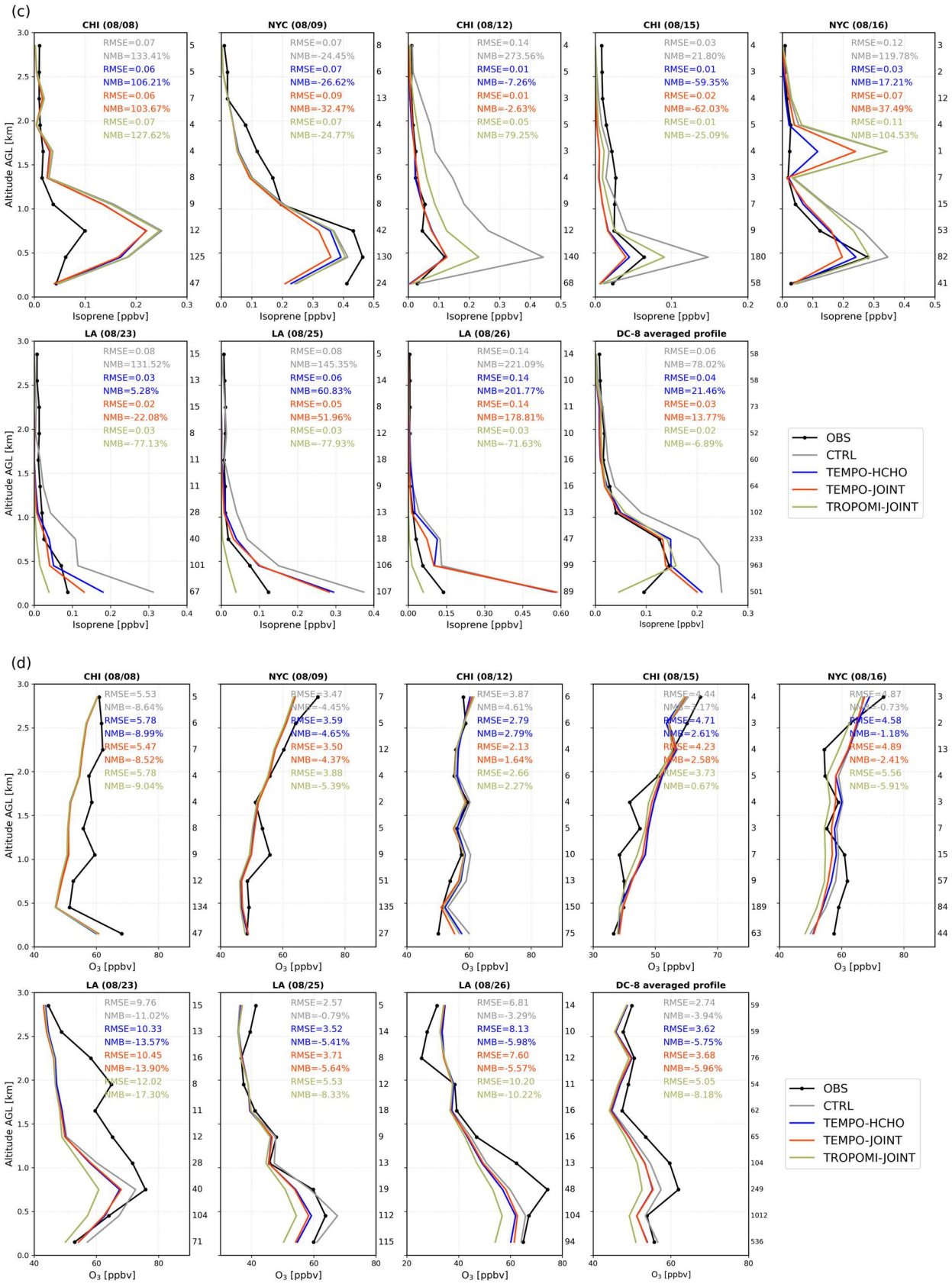

(c)
CHI (08/08)
RMSE=0.07
NMB=133.41%
RMSE=0.06
NMB=106.21%
RMSE=0.06
NMB=103.67%
RMSE=0.07
NMB=127.62%
NYC (08/09)
RMSE=0.07
NMB=-24.45%
RMSE=0.07
NMB=-26.62%
RMSE=0.09
NMB=-32.47%
RMSE=0.07
NMB=-24.77%
CHI (08/12)
RMSE=0.14
NMB=273.56%
RMSE=0.01
NMB=-7.26%
RMSE=0.01
NMB=-2.63%
RMSE=0.05
NMB=79.25%
CHI (08/15)
RMSE=0.03
NMB=21.80%
RMSE=0.01
NMB=-59.35%
RMSE=0.02
NMB=-62.03%
RMSE=0.01
NMB=-25.09%
NYC (08/16)
RMSE=0.12
NMB=119.78%
RMSE=0.03
NMB=17.21%
RMSE=0.07
NMB=37.49%
RMSE=0.11
NMB=104.53%
LA (08/23)
RMSE=0.08
NMB=131.52%
RMSE=0.03
NMB=5.28%
RMSE=0.02
NMB=-22.08%
RMSE=0.03
NMB=-77.13%
LA (08/25)
RMSE=0.08
NMB=145.35%
RMSE=0.06
NMB=60.83%
RMSE=0.05
NMB=51.96%
RMSE=0.03
NMB=-77.93%
LA (08/26)
RMSE=0.14
NMB=221.09%
RMSE=0.14
NMB=201.77%
RMSE=0.14
NMB=178.81%
RMSE=0.03
NMB=-71.63%
DC-8 averaged profile
RMSE=0.06
NMB=78.02%
RMSE=0.04
NMB=21.46%
RMSE=0.03
NMB=13.77%
RMSE=0.02
NMB=-6.89%
Altitude AGL [km]
Isoprene [ppbv]
OBS
CTRL
TEMPO-HCHO
TEMPO-JOINT
TROPOMI-JOINT
(d)
CHI (08/08)
RMSE=5.53
NMB=-8.64%
RMSE=5.78
NMB=-8.99%
RMSE=5.47
NMB=-8.52%
RMSE=5.78
NMB=-9.04%
NYC (08/09)
RMSE=3.47
NMB=-4.45%
RMSE=3.59
NMB=-4.65%
RMSE=3.50
NMB=-4.37%
RMSE=3.88
NMB=-5.39%
CHI (08/12)
RMSE=3.87
NMB=4.61%
RMSE=2.79
NMB=2.79%
RMSE=2.13
NMB=1.64%
RMSE=2.66
NMB=2.27%
CHI (08/15)
RMSE=4.44
NMB=-5.17%
RMSE=4.71
NMB=2.61%
RMSE=4.23
NMB=2.58%
RMSE=3.73
NMB=0.67%
NYC (08/16)
RMSE=4.87
NMB=-0.73%
RMSE=4.58
NMB=-1.18%
RMSE=4.89
NMB=-2.41%
RMSE=5.56
NMB=-5.91%
LA (08/23)
RMSE=9.76
NMB=-11.02%
RMSE=10.33
NMB=-13.57%
RMSE=10.45
NMB=-13.90%
RMSE=12.02
NMB=-17.30%
LA (08/25)
RMSE=2.57
NMB=-0.79%
RMSE=3.52
NMB=-5.41%
RMSE=3.71
NMB=-5.64%
RMSE=5.53
NMB=-8.33%
LA (08/26)
RMSE=6.81
NMB=-3.29%
RMSE=8.13
NMB=-5.98%
RMSE=7.60
NMB=-5.57%
RMSE=10.20
NMB=-10.22%
DC-8 averaged profile
RMSE=2.74
NMB=-3.94%
RMSE=3.62
NMB=-5.75%
RMSE=3.68
NMB=-5.96%
RMSE=5.05
NMB=-8.18%
Altitude AGL [km]
O3 [ppbv]
OBS
CTRL
TEMPO-HCHO
TEMPO-JOINT
TROPOMI-JOINT

Figure S5. Average model simulated and DC-8 observed trace gas vertical profile for individual flight days. (a) NO_x, (b) HCHO, (c) isoprene, and (d) O_3.

Reference

Anderson, J. L. (2007). An adaptive covariance inflation error correction algorithm for ensemble filters. *Tellus Series A-Dynamic Meteorology and Oceanography*, 59(2), 210–224. https://doi.org/10.1111/j.1600-0870.2006.00216.x

Boccippio, D. J., Cummins, K. L., Christian, H. J., & Goodman, S. J. (2001). Combined satellite- and surface-based estimation of the Intracloud–Cloud-to-Ground Lightning Ratio over the Continental United States. *Monthly Weather Review*, 129(1), 108–122. https://doi.org/10.1175/15

Grell, G. A., & Dévényi, D. (2002). A generalized approach to parameterizing convection combining ensemble and data assimilation techniques. *Geophysical Research Letters*, 29(14), 38–1. https://doi.org/10.1029/2002gl015311

Hong, S. Y., Dudhia, J., & Chen, S. H. (2004). A Revised Approach to Ice Microphysical Processes for the Bulk Parameterization of Clouds and Precipitation. *Monthly Weather Review*, 132(1), 103–120. Retrieved from http://dx.doi.org/10.1175/1520-0493(2004)132<0103:aratim>2.0.co;2

Miyazaki, K., Eskes, H. J., & Sudo, K. (2012). Global NO_x emission estimates derived from an assimilation of OMI tropospheric NO_2 columns. *Atmospheric Chemistry and Physics*, 12(5), 2263–2288. https://doi.org/10.5194/acp-12-2263-2012

Mlawer, E. J., Taubman, S. J., Brown, P. D., Iacono, M. J., & Clough, S. A. (1997). Radiative transfer for inhomogeneous atmospheres: RRTM, a validated correlated-k model for the longwave. Journal of Geophysical Research: Atmospheres, 102(D14), 16663–16682. https://doi.org/10.1029/97jd00237

Mukul Tewari, N., Tewari, M., Chen, F., Wang, W., Dudhia, J., LeMone, M., et al. (2004). Implementation and verification of the unified NOAH land surface model in the WRF model. Presented at the 20th conference on weather analysis and forecasting/16th conference on numerical weather prediction(Formerly Paper Number 17.5) (pp. 11–15).

Nakanishi, M., & H. Niino (2009). Development of an Improved Turbulence Closure Model for the Atmospheric Boundary Layer. *Journal of the Meteorological Society of Japan*. Ser. II, 87(5), 895–912. https://doi.org/10.2151/jmsj.87.895

Pierce, R. B., Al-Saadi, J. A., Schaack, T., Lenzen, A., Zapotocny, T., Johnson, D., et al. (2003). Regional Air Quality Modeling System (RAQMS) predictions of the tropospheric ozone budget over east Asia. *Journal of Geophysical Research Atmospheres*, *108*(D21). https://doi.org/10.1029/2002jd003176